Reactions of Diborane with Ammonia and Ammonia Borane: Catalytic Effects for Multiple Pathways for Hydrogen Release

Vinh Son Nguyen,[‡] Myrna H. Matus,[†] Minh Tho Nguyen,*[,†,‡] and David A. Dixon*[,†]

Department of Chemistry, The University of Alabama, Shelby Hall, Tuscaloosa, Alabama 35487-0336, and Department of Chemistry, University of Leuven, B-3001 Leuven, Belgium

Received: May 28, 2008; Revised Manuscript Received: July 16, 2008

High-level electronic structure calculations have been used to construct portions of the potential energy surfaces related to the reaction of diborane with ammonia and ammonia borane ($B_2H_6 + NH_3$ and $B_2H_6 + BH_3NH_3$) to probe the molecular mechanism of H_2 release. Geometries of stationary points were optimized at the MP2/aug-cc-pVTZ level. Total energies were computed at the coupled-cluster CCSD(T) theory level with the correlation-consistent basis sets. The results show a wide range of reaction pathways for H_2 elimination. The initial interaction of $B_2H_6 + NH_3$ leads to a weak preassociation complex, from which a B−H−B bridge bond is broken giving rise to a more stable $H_3BHBH_2NH_3$ adduct. This intermediate, which is also formed from $BH_3NH_3 + BH_3$, is connected with at least six transition states for H_2 release with energies 18−93 kcal/mol above the separated reactants. The lowest-lying transition state is a six-member cycle, in which BH_3 exerts a bifunctional catalytic effect accelerating H_2 generation within a B−H−H−N framework. Diborane also induces a catalytic effect for H_2 elimination from BH_3NH_3 via a three-step pathway with cyclic transition states. Following conformational changes, the rate-determining transition state for H_2 release is ∼27 kcal/mol above the $B_2H_6 + BH_3NH_3$ reactants, as compared with an energy barrier of ∼37 kcal/mol for H_2 release from BH_3NH_3. The behavior of two separated BH_3 molecules is more complex and involves multiple reaction pathways. Channels from diborane or borane initially converge to a complex comprising the $H_3BHBH_2NH_3$ adduct plus BH_3. The interaction of free BH_3 with the BH_3 moiety of BH_3NH_3 via a six-member transition state with diborane type of bonding leads to a lower-energy transition state. The corresponding energy barrier is ∼8 kcal/mol, relative to the reference point $H_3BHBH_2NH_3$ adduct + BH_3. These transition states are 27−36 kcal/mol above $BH_3NH_3 + B_2H_6$, but 1−9 kcal/mol *below* the separated reactants $BH_3NH_3 + 2\ BH_3$. Upon chemical activation of B_2H_6 by forming 2 BH_3, there should be sufficient internal energy to undergo spontaneous H_2 release. Proceeding in the opposite direction, the H_2 regeneration of the products of the $B_2H_6 + BH_3NH_3$ reaction should be a feasible process under mild thermal conditions.

Introduction

Diborane (B_2H_6, **db**) dissociates slowly at room temperature in the absence of moisture or lubricants.[1] It can be conveniently prepared in pure form and is used as a reagent for a variety of syntheses. The presence of the bridge B−H−B bond in **db** constituted the basis for a novel rationalization and theory for the molecular structure of the boranes and carboranes.[2] Stock and Kuss[3] reported in 1923 the reaction of **db** with ammonia, in which **db** was shown to take up two molecules of ammonia to form a salt. On heating the resulting "diammoniate of diborane" salt (**dadb**) in a closed tube up to 200 °C, a considerable amount of $B_3N_3H_6$ was produced.[4] The latter was confirmed to have a six-member ring structure by electron diffraction[5] (this cyclic compound analogous to benzene was first named "triborine triamine"[6] and later named "borazine"). The salt was initially proposed to be $[B_2H_4^{2-}][NH_4^+]_2$, whose solution was found to have a low electric conductivity.[1,7] Subsequently, Schlesinger and co-workers[8] interpreted the reaction as an initial addition of borane (BH_3, **B**, formed from bond cleavage of **db**) to ammonia (**A**), followed by other reactions leading to a final product ion pair product $[H_3BNH_2BH_3^-][NH_4^+]$. The other ion pair alternative $[H_3NBH_2NH_3^+][BH_4^-]$ was not considered in these early reports. During the course of the **db** + **A** reaction, small quantities of a new volatile compound having the molecular formula (B_2H_7N) were identified,[8] and the latter compound was subsequently obtained in high yield by passing an excess of **db** over the salt.[9] The (B_2H_7N) compound formally corresponds to the product of an elimination of H_2 from the **db** + **A** reactants. The diborane plus ammonia reaction remains one of the ways of preparing borazine and is a precursor for the epitaxial growth of boron nitride thin films on a silicon substrate by chemical vapor deposition (CVD).[10−12] When a mixture of **db** and **A** was passed through a heated quartz tube in a gas-phase pyrolysis process, aminoborane H_2BNH_2 is formed and has been characterized by Sugie et al.[13] using microwave spectroscopy (T = 500 °C) and by Carpenter and Ault[14] using matrix isolation infrared spectroscopy (T = 360 °C).

McKee[15] probed the molecular mechanism of this gas-phase process by exploring a portion of the relevant potential energy surface (PES) at the MP4/6-31+G(2d,p)//MP2(6-31G(d) + ZPE level of ab initio molecular orbital theory (his energy profiles are shown in Figure S1 of the Supporting Information). He found the following: (i) the initial addition of ammonia to **db** yielding a $B_2H_6NH_3$ adduct is prohibited by a non-negligible energy barrier; (ii) the adduct having a B−H−B bridged bond is the common adduct of the barrier-free condensation of ammonia

* Corresponding authors. E-mail: dadixon@as.ua.edu (D.A.D.).
‡ University of Leuven.
† The University of Alabama.

10.1021/jp804714r CCC: $40.75
Published on Web 09/04/2008

borane (BH_3NH_3, **ab**) to BH_3; (iii) the structure of the transition state (TS) for H_2 release from $B_2H_6NH_3$ is that for the unimolecular release of H_2 from BH_3NH_3 (via 1,2-H_2 elimination) plus a destabilizing interaction with the second BH_3 molecule; and (iv) there is an overall increase of 6.4 kcal/mol for the energy barrier for H_2 formation, relative to that in BH_3NH_3. The rate-determining TS was calculated to be 42.4 kcal/mol above the separated **db** + **A** reactants.[15] This value is above the calculated 0 K enthalpy for dissociation of B_2H_6 into two BH_3 molecules of 38.1 kcal/mol.[16] In subsequent studies, Sakai[17,18] proposed a different mechanism for BH_2NH_2 formation in the reaction **db** + **A**, which basically involves the same initial adduct but instead undergoes H_2 loss through a six-member cyclic TS (Supporting Information Figure S2, ESI). At the MP4/6-31G(d,p)//MP2/6-31G(d,p) + ZPE level, this cyclic TS is ~17 kcal/mol above the separated reactants. The favorable HOMO−LUMO interaction was identified as a stabilizing factor of the cyclic TS.[17]

We[19,20] have extensively investigated H_2 release starting from the **ab** + **B** reactants, with coupled-cluster CCSD(T) theory using the aug-cc-pV*n*Z (n = D, T, Q) basis sets extrapolated to the complete basis set limit. We confirmed the initial formation of the monobridged B−H−B complex which is the same complex formed from **db** + **A**. From this common complex we found three different channels for H_2 elimination, which included the paths found earlier by McKee[15] and Sakai.[17,18] Our high-accuracy results agreed with Sakai demonstrating the low-energy pathway via the six-member cyclic TS, and we pointed out the role of the second borane molecule, which acts as a Lewis acid bifunctional catalyst for H_2 release from **ab**, and its potential use in the perspective of chemical hydrogen storage for transportation sector.[21−26] Ammonia was also found to provide a catalytic effect on H_2 elimination from **ab** through a cyclic six-member TS containing a N−H−H−B framework,[19] but the overall reduction of the energy barrier by ammonia is smaller, and the Lewis base NH_3 is a less effective catalyst than the Lewis acid BH_3. A substituted diborane intermediate has been proposed to react with imidazole-borane in the formation of the condensation polymer of imidazole-borane with loss of hydrogen.[27]

When constructing the PES of the **ab** + **B** reaction,[19] we did not consider the channels involving **db**. The available results[15,17,19,20] are somewhat incomplete, and a global view of the processes in this important region of the PES is still missing. We have further explored the regions of the PES for both the B_2H_6 + NH_3 and BH_3NH_3 + BH_3 channels using a uniform high level of theory. Because borane can act as a Lewis acid catalyst for H_2 formation, two questions are (i) can diborane act as such a catalyst, and (ii) do two separated borane molecules reinforce the catalytic effect? To address these questions, we have studied the PES describing the reaction of ammonia borane with diborane BH_3NH_3 + B_2H_6, and ammonia borane with two borane molecules BH_3NH_3 + $2BH_3$.

Computational Methods

The calculations were performed by using the Gaussian-03[28] and MOLPRO[29] suites of programs. The geometry parameters were initially optimized using second-order perturbation theory (MP2)[30] in conjunction with the correlation-consistent aug-cc-pVDZ basis set.[31] The character of each stationary point was determined to be an equilibrium structure or a first-order saddle point, by calculations of harmonic vibrational frequencies at the same level. To ascertain the identity of each TS, intrinsic reaction coordinate (IRC)[32] calculations were systematically

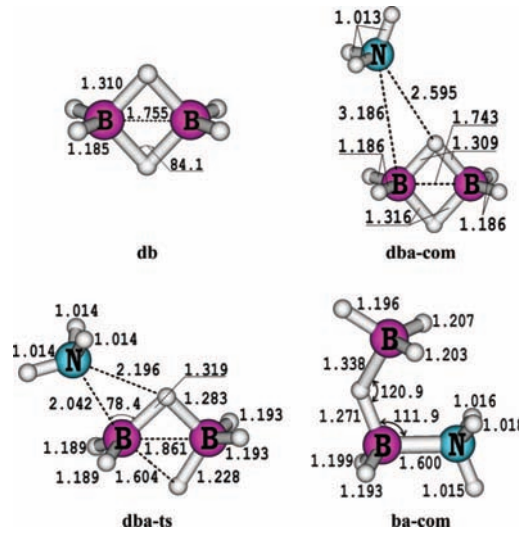

Figure 1. Selected MP2/aVTZ geometry parameters of **db**, **dba-com**, **ba-com**, and transition state structure (TS), **dba-ts**. Bond distances in are angstroms, and bond angles are in degrees.

carried out at the MP2/aVDZ level. Geometry parameters of relevant structures were then reoptimized using the MP2 method with the larger aug-cc-pVTZ basis set (denoted hereafter as aV*n*Z, with n = D and T). The latter optimized geometries were subsequently utilized for single-point electronic energies using coupled-cluster CCSD(T) theory with the same basis set.[33] In all of the MP2 and CCSD(T) calculations, the core orbitals were kept frozen. The zero-point energies (ZPEs) were calculated by using MP2/aVDZ harmonic vibrational frequencies scaled by a factor of 0.9787 for boron hydrides (B_nH_m) and 0.9876 for ammonia borane derivatives. The scaling factors were derived from previous evaluations of the ZPEs for B_2H_6[16,34] and BH_3NH_3.[25] Due to the large number of structures considered, the PESs considered were constructed using CCSD(T)/aVTZ electronic energies with the appropriate ZPE corrections. In our previous studies,[19,20,35] we have shown that the relative energies obtained at this level of theory deviate by about ±1.0 kcal/mol with respect to the values obtained by CCSD(T)/CBS + ZPE calculations, in which the coupled-cluster energies were extrapolated to the complete basis set limit for these types of reactions. A slightly larger deviation of 1.6 kcal/mol is found for the dimerization energy of $2BH_3 \rightarrow B_2H_6$. Unless otherwise noted, the relative energies quoted hereafter refer to the CCSD(T)/aVTZ + ZPE results.

Results and Discussion

Table S1 of the Supporting Information lists the total and ZPEs of all the stationary points considered and imaginary frequencies of the TSs. Supporting Information Table S2 lists the relative energies for the stationary points related to the B_2H_6 + NH_3 reaction for Figure 3, Table S3 of the Supporting Information lists those for the BH_3NH_3 + B_2H_6 reaction for Figure 6, and Table S4 of the Supporting Information lists those for the BH_3NH_3 + B_2H_6 reaction for Figure 7, all calculated at the MP2/aVDZ, CCSD(T)/aVDZ, and CCSD(T)/aVTZ + ZPE levels. Supporting Information Table S5 describes the Cartesian coordinates of MP2/aVTZ optimized geometries, and Figures S3 and S4 of the Supporting Information display the shape and selected geometrical parameters of the structures not shown in the text.

Reaction Pathways for H_2 Release from B_2H_6 + NH_3 (db + A). The structures of the most relevant stationary points, along with selected MP2/aVTZ geometrical parameters, are given in

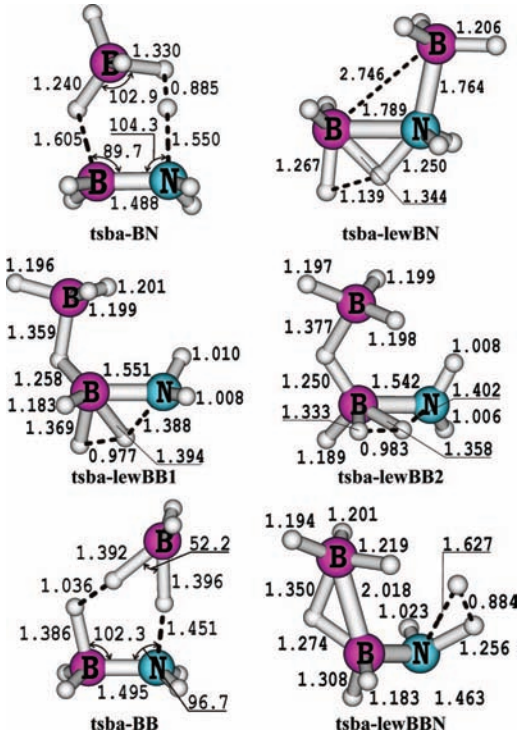

Figure 2. Selected MP2/aVTZ geometry parameters of transition state structures (TS) for H_2 elimination from **ba-com**. Bond distances are in angstroms, and bond angles are in degrees.

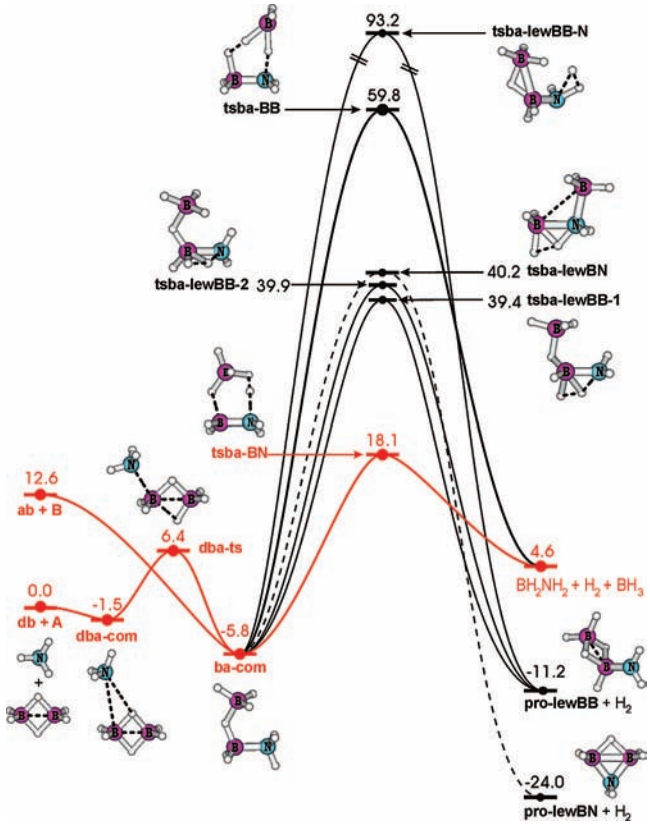

Figure 3. Schematic energy profiles illustrating different reaction pathways for H_2 release from diborane + ammonia **db** + **A**. Relative energies are in kcal/mol from CCSD(T)/aVTZ + ZPE calculations. The red profiles are the lowest-energy pathways.

Figures 1 and 2. A few stationary points have already been given in our previous study of the **ab** + **B** reaction,[19] so to facilitate comparison, we keep, where possible, the same labeling as for

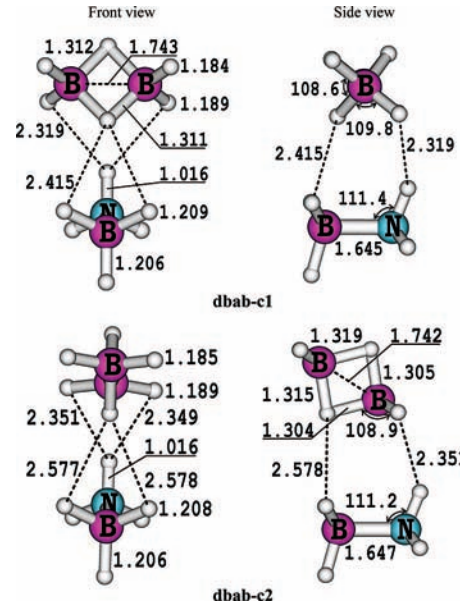

Figure 4. Selected MP2/aVTZ geometry parameters of two complexes **dbab-c1** (perpendicular) and **dbab-c2** (planar) between diborane and ammonia borane **db** + **ab**. Bond distances are in angstroms, and bond angles are in degrees.

the structures already reported. These are the adduct **ba-com** and some TSs connecting it to different products. Profiles for relative energies along the reaction pathways are illustrated in Figure 3.

Starting from the reactants **db** + **A**, we find a weak interaction between the N lone pair and the bridged B−H bond, which leads to formation of the complex, **dba-com**. This first step is barrier-free with a small complexation energy. There are small changes in **dba-com** with respect to the geometry of **db** (Figure 1). The two B−H−B bridged bonds are slightly distorted, 0.006 Å, from **db** to **dba-com**. The B−B distance in **dba-com** shortens relative with respect to that in **db**, by 0.012 Å. In comparison with previous work,[15,17,18] **dba-com** represents a new complex for the reaction of diborane with ammonia.

dba-com rearranges to **ba-com** via TS **dba-ts**, only 6.4 kcal/mol above the reactants. **dba-ts** is the same as the TS reported earlier by Sakai,[17] and his energy barrier computed at a lower level differs by +3.0 kcal/mol from our value. The geometry parameters (Figure 1) show that **dba-ts** is formed by a nearly perpendicular approach of the NH_3-nitrogen to a B atom of diborane. The NH_3 group moves out of the plane containing the bridged B−B/B−H bonds. The attack of N to one B−H bridge bond breaks another bond from the opposite side and opens the diborane framework forming a BH_3-type fragment (cf., Figure 1). IRC calculations in both the forward and reverse directions from **dba-ts** confirm its connection to both complexes. **ba-com** can be reached by free rotation of BH_3 around the B−H axis. **ba-com** has been shown to be the common adduct of **ab** and **B**.[19] We note that this complex contains only one bridge B−H−B bond and the B−H distance differs by 0.4 Å from that in diborane. **ba-com** is lower in energy than **dba-com**.

Starting from **ba-com**, H_2 elimination can occur through at least six TSs associated with a range of energy barriers from 18 to 93 kcal/mol with respect to the reactants **db** + **A**. In our previous work,[19] only three TSs were reported. On the basis of the role of BH_3 group, we can divide the six TSs into three different types. In the first type, BH_3 plays an active role in H_2 formation by donating and receiving H atoms. These include **tsba-BN** and **tsba-BB** discussed previously.[19] In Figure 3, the

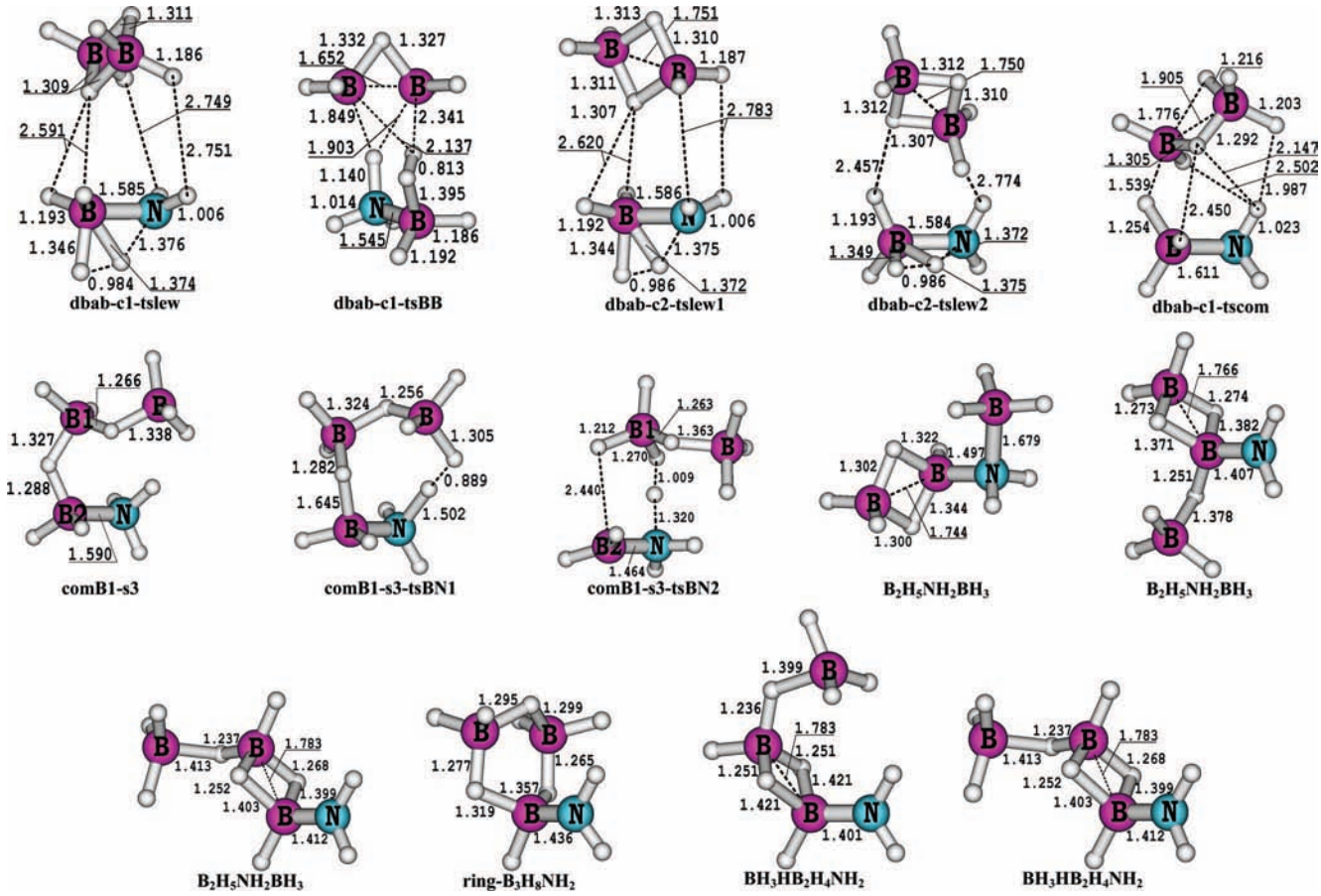

Figure 5. Selected MP2/aVTZ geometry parameters of six TSs related to the reaction of diborane + ammonia borane **db** + **ab** and an intermediate complex. Bond distances are in angstroms, and bond angles are in degrees.

lowest-energy pathway, **tsba-BN**, is drawn in a bold red line. The most important difference between the pathways through **tsba-BN** and **tsba-BB** is the way in which the departing H_2 is formed. In the former, the H_2 is lost from the N and the attacking BH_3, and in the latter, it is lost from B and the attacking BH_3. The energy barrier through **tsba-BN** is 41.7 kcal/mol smaller than that via **tsba-BB**. Such a difference, larger than the dissociation energy of diborane to separated BH_3 molecules (38.1 kcal/mol at 0 K),[16] exhibits itself in substantial differences in the character of both TSs. In **tsba-BN**, the B−H−B bridged bond remains and the H_2 is formed within a B−H−H−N framework. In contrast, the B−H−H−B bonds in **tsba-BB** are disfavored by the repulsive charge distributions on the two reacting negative B−H bonds. As shown by the IRC analysis, both TSs connect to the same products $BH_2NH_2 + BH_3 + H_2$, 4.6 kcal/mol above the reactants.

We found four TSs in which the BH_3 group has the role of a classical Lewis acid. The letter **tsba-lew** is used to designate this type of TS, with **lew** standing for a Lewis type of interaction. Dependent on the position (B or N in BH_3NH_3) where the B atom of BH_3 is attached to, the labels **tsba-lewBB** and **tsba-lewBN** are used. Attachment of B to N results in **tsba-lewBN**, which is the only TS found for this type and has been described previously (dashed line in Figure 3).[19] This TS is calculated to be at 22.1 kcal/mol above **tsba-BN** and gives rise to the most stable cyclic product **pro-lewBN**.

Attachment of B to B leads to the third type of TS and includes three TSs named **tsba-lewBB-1**, **tsba-lewBB-2**, and **tsa-lewBB-N** (Figure 3). The numbers 1 and 2 indicate two different positions of the departing H_2 with regard to the attaching BH_3 group. The H_2 release from the back-side **tsba-lewBB-1** occurs with a dihedral angle BBNH of 112°. **tsba-lewBB-2** is formed by a bridged B−H−B bond at the lateral-side position of BH_3NH_3, with a dihedral angle BBNH of only 3°. Both TSs describe the same kind of H_2 release from BH_3NH_3 with H-transfer from NH_3 to a B atom accompanied by an elongation of a B−H bond giving H_2.[19] Both TSs have a similar energy content, with a difference of only 0.5 kcal/mol in favor of **tsba-lewBB-1**. As seen in Figure 3, all three TSs lead to the same product **pro-lewBB**, as confirmed by their IRC pathways. This product $BH_3NH_2BH_2$ (aminodiborane) + H_2 is more stable than **db** + **A**.

The letter **N** in **tsba-lewBB-N** stands for H_2 departure from two H atoms of NH_3. This TS is given only for the sake of completeness, because due to the breaking of two NH bonds, it is located at the highest-energy position above **db** + **A** and is not significant.

The results summarized in Figure 3 show that, at an early stage, both **db** + **A** and **ab** + **B** channels converge to the common adduct **ba-com** which plays a key role for the entire transformation. The calculated energy barriers range from 18.1 to 93.2 kcal/mol relative to **db** + **A**. With respect to the results reported in our previous study,[19] the three additional TSs remain substantially higher in energy than **tsba-BN**. Therefore, they do not affect the conclusions already drawn concerning the reaction **ab** + **B**, where we note again the important role of the borane molecule as a Lewis acid catalyst for H_2 release. The current results complete the PES for H_2 release and directly link the two starting systems, $BH_3NH_3 + BH_3$ and $B_2H_6 + NH_3$.

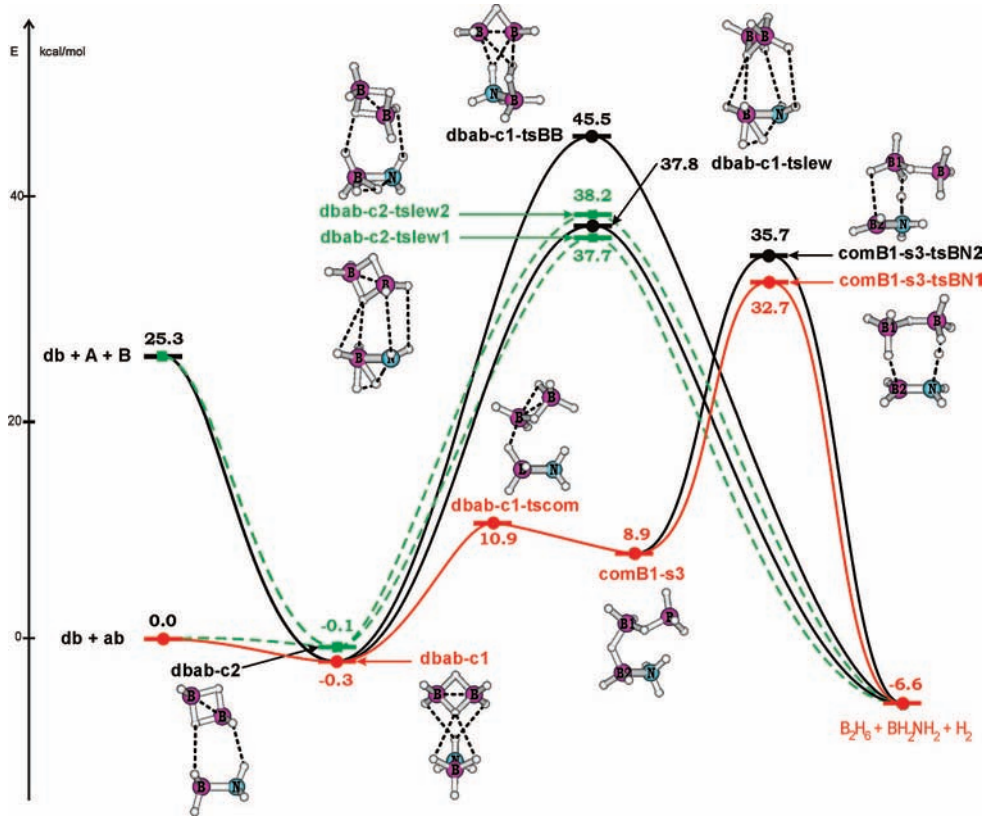

Figure 6. Schematic energy profiles of pathways for rearrangement and H_2 release from two complexes between diborane plus ammonia borane **db** + **ab**. Relative energies are in kcal/mol from CCSD(T)/aVTZ + ZPE calculations. The red profiles are the lowest-energy pathways.

For the diborane plus ammonia reaction, our current results that **tsba-BN** is only 18.1 kcal/mol above the reactants **db** + **A** are in agreement with experimental studies[12−14] showing production of gaseous aminoborane (BH_2NH_2) upon thermal decomposition of BH_3NH_3 under mild conditions. This provides us with further support for H_2 release from BH_3NH_3 in the presence of the catalyst BH_3 passing through the six-member cyclic TS **tsba-BN**. Proceeding in an opposite direction with a reaction beginning from $BH_2NH_2 + H_2 + BH_3$, or from the adduct **ba-com**, if available, leads to formation of diborane.

Reaction Pathways from B_2H_6 + BH_3NH_3 (db + ab). In our search for lower energy H_2 release processes, we have investigated the reaction between diborane and ammonia borane **db** + **ab** to determine if diborane can act as a catalyst for H_2 release from ammonia borane. The initial interaction between **db** and **ab** gives rise to two relatively weak complexes having the same type of long B−H−H−B and B−H−H−N bonds, but with different orientations. The complexes are referred to as **dbab-c1** and **dbab-c2**, in which the letter **c** denotes a complex and the number their relative stability. Figure 4 shows selected geometry parameters in both front and side views of their equilibrium structures. The complexation energies of **dbab-c1** and **dbab-c2** are <0.5 kcal/mol with respect to the reactants, respectively, and may or may not exist at higher levels of theory. The pair of complexes is connected by almost free rotation of NH_3 around the BHHB skeleton. **dbab-c1** results from a nearly perpendicular approach between the two monomers. This complex has two weak B−H−H−B and B−H−H−N interactions. **dbab-c2** is characterized by an arrangement with all B and N atoms of both monomers in the same plane. The H−H distances within the B−H−H−N dihydrogen bond are longer than those of **dbab-c1** by 0.04−0.16 Å.

The geometry parameters for the relevant TSs and product are shown in Figure 5, and the schematic potential energy profiles for H_2 release are illustrated in Figure 6. We located four TSs for direct H_2 elimination, which can be divided into two types. The first type of TS starts from **dbab-c1** and **dbab-c2** and includes **dbab-c1-tslew**, **dbab-c2-tslew1**, and **dbab-c2-tslew2** (Figure 5). **dbab-c1-tslew** is a TS for H_2 elimination from the BH_3NH_3 group within **dbab-c1**. It is built from interactions between B_2H_6 with the TS for loss of H_2 from BH_3NH_3 via weak dihydrogen-bridged B−H−H−B and B−H−H−N bonds. The position of B_2H_6 is still perpendicular to the BH_3NH_3 group as in **dbab-c1**. The B−H, N−H, B−N, and H−H distances in the **ab** group are similar to those of the BH_3NH_3 monomer, which was analyzed in detail previously.[19] In comparison with the corresponding values in **dbab-c1**, the H−H distances in **dbab-c1-tslew** are elongated by 0.18−0.44 Å, whereas the B−H and N−H distances are slightly compressed. The energy of **dbab-c1-tslew** is 37.8, 38.1, and 12.5 kcal/mol above the reactants **db** + **ab**, **dbab-c1**, and **db** + **A** + **B**, respectively.

Similarly, **dbab-c2-tslew1** is formed by two B−H−H−B and B−H−H−N interactions between B_2H_6 and the BH_3NH_3 monomer TS. All of the heavy atoms are again in a plane. The changes in the B−H, N−H, and H−H distances within the dihydrogen bridges B−H−H−B and B−H−H−N are not large (∼0.04 Å) as compared to **dbab-c2**. **dbab-c2-tslew1** is only 0.1 kcal/mol below **dbab-c1-tslew** and **dbab-c2-tslew2** is only 0.5 kcal/mol higher in energy than **dbab-c2-tslew1**. In contrast to **dbab-c2-tslew1**, formation of **dbab-c2-tslew2** has only one B−H−H−B and one B−H−H−N dihydrogen bond with the BH_3NH_3 monomer TS. The H−H distances in **dbab-c2-tslew2** are shorter by 0.1−0.4 Å than those of **dbab-c2-tslew1**. Molecular H_2 is generated in a plane nearly perpendicular to that containing the heavy atoms (<BBNB = 2.3°). IRC calculations confirm that the products from these three different TSs are the $B_2H_6 + BH_2NH_2 + H_2$ fragments.

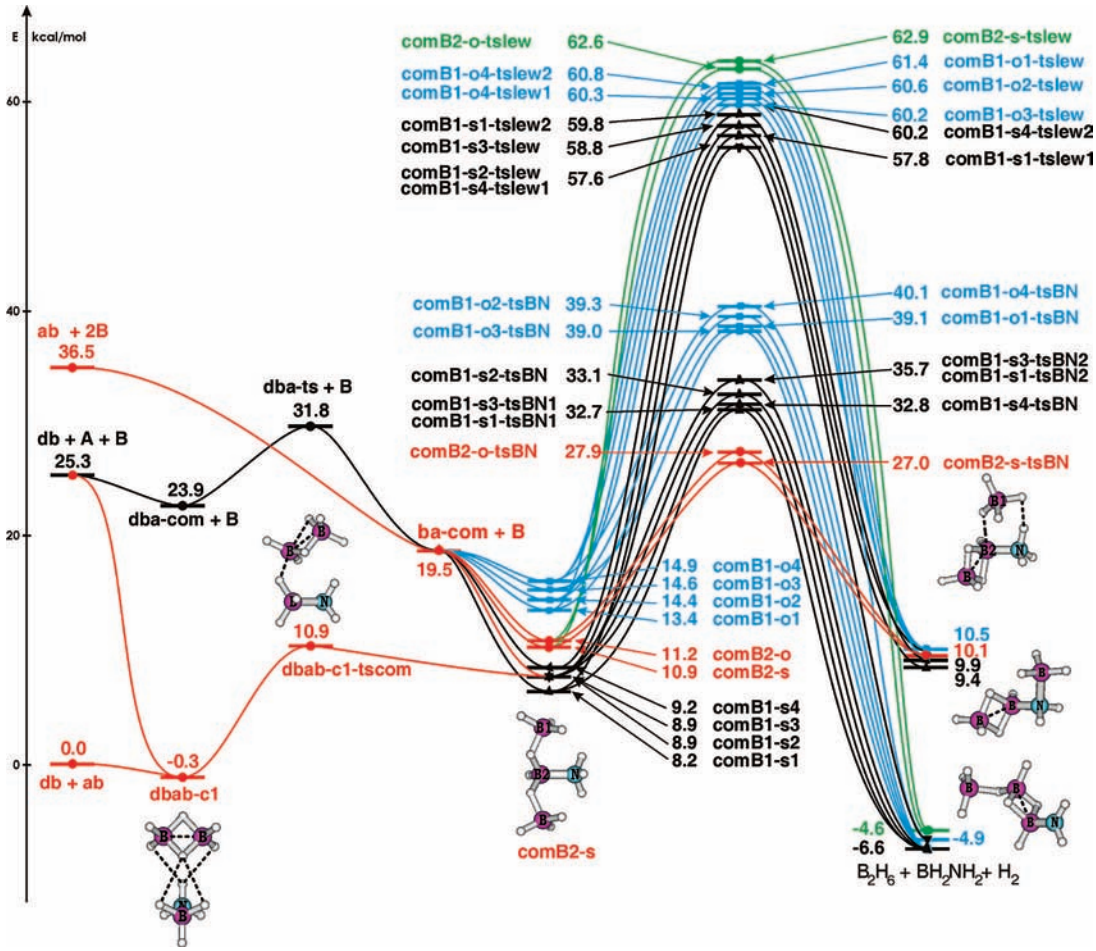

Figure 7. Schematic energy profiles illustrating pathways for H_2 release from ammonia borane plus two boranes **ab** + 2**B**. Relative energies are in kcal/mol obtained from CCSD(T)/aVTZ + ZPE calculations. The red profiles are the lowest-energy pathways. $\Delta E(B_2H_6 + BH_2NH_2 + H_2) = -6.6$, $\Delta E(B_2H_5NH_2BH_3 + H_2) = 10.1$, $\Delta E(\text{ring-}B_3H_8NH_2 + H_2) = 9.9$, $\Delta E(BH_3HB_2H_4NH_2 + H_2) = 9.4$, $\Delta E(B_2H_6NH_2BH_2 + H_2) = 10.5$, $\Delta E(B_2H_4HBH_3NH_2 + H_2) = -4.6$, and $\Delta E(B_2H_4HBH_3NH_2 + H_2) = -4.9$ kcal/mol.

The second type of TS, which originates from **dbab-c1**, is **dbab-c1-tsBB** (Figures 5 and 6). As above, the letter **BB** stands for a H_2 loss from two B atoms. Formation of H_2 is characterized by a combination of one H atom from the bridge B−H−B bond in B_2H_6 and another H atom from a B−H bond of BH_3NH_3. The B−H bond in BH_3NH_3 from which an H atom is lost is longer than the other by ∼0.2 Å. The N−H bonds, which interact with B_2H_6, are elongated by ∼0.13 Å. Breaking a B−H−B bond and shortening of B−H bonds in B−H−H−N interactions make it more difficult to form **dbab-c1-tsBB**. **dbab-c1-tsBB** is ∼8 kcal/mol higher in energy than the two previous TSs. The products from this TS are $B_2H_6 + BH_2NH_2 + H_2$. This TS can be compared with TS **tsba-BB** (Figure 2). Relative to **tsba-BB**, the energy barrier via **dbab-c1-tsBB** is reduced from 65.7 to 45.8 kcal/mol with respect to the relevant prereaction complexes.

H_2 elimination from **dbab-c1** can proceed via two-step pathways. The first step is formation of the intermediate **comB1-s3** through TS **dbab-c1-tscom**. The second step is H_2 elimination from **comB1-s3**, via two different TSs: **comB1-s3-tsBN1** and **comB1-s3-tsBN2**. Intermediate **comB1-s3** is calculated to be 8.9 kcal/mol above the reactants **db** + **ab**; the diborane moiety is partially disrupted with only one B−H−B1 bridge, and a new B1−H−B2 bridge forms connecting **ab** and **db**. In TS **dbab-c1-tscom**, the B−H distances indicate bond cleavage. The attack of B(**db**) on H of BH_3(**ab**) induces four weak B−H−H−B and B−H−H−N bonds (cf., Figure 5). These numerous interactions tend to stabilize **dbab-c1-tscom**, so it is only 10.9 kcal/mol above the reactants **db** + **ab**. IRC calculations along the forward direction result in **comB1-s3** (Figure 6).

Although TS **dbab-c1-tscom** is of low-energy, TS **comB1-s3-tsBN1** and **TS comB1-s3-tsBN2**, involving H_2 formation from B−H−H−N, are much higher in energy. **comB1-s3-tsBN1** is an eight-member ring forming H_2 from a B−H bond of terminal borane. **comB1-s3-tsBN2** is a six-member ring in which H_2 is formed from an internal borane B−H bond (of diborane). It appears that the two-step H_2 release is ∼5 kcal/mol favored over the one-step pathway. In addition, the intermediate **comB1-s3** links to another region of the PES as described in the following section.

The results summarized in Figure 6 show how diborane affects the H_2 release reaction. **db** can behave as a conventional Lewis acid interacting with the TS for H_2 release from ammonia borane. This interaction does not happen via BB or BN bonds but rather via dihydrogen-bridged bonds which can stabilize the TS. In comparison to the previous results[18,19] on the energy barriers for H_2 elimination, this type of approach is not significant: 36.8 kcal/mol for **ab**, 5.5 kcal/mol for **ab** + **B** (Figure 3), and for **ab** + **db**, 37.7 kcal/mol via the one-step pathway, and 32.7 kcal/mol via the two-step pathway (energies for the same type of effect relative to separated reactants). Starting from the weak preassociation complexes does not change the energetics. In this pathway, even though the bridge

B−H−B bonds are not broken, the energy of the TS is still high. We conclude that diborane, when reacting as a stable and compact entity, exerts a small catalytic effect for H_2 release of ammonia borane, in reducing the energy barrier by ∼4 kcal/mol from the BH_3NH_3 monomer to the B_2H_6 + BH_3NH_3 reaction involving a two-step pathway via TS **comB1-s3-tsBN1**. Thus, B_2H_6 is not a catalyst as effective as BH_3.

H_2 Release from Reactions of Ammonia Borane with Two Borane Molecules (ab + 2B). As discussed above, the adduct **ba-com** ($BH_3HBH_2NH_3$) is formed either from a direct combination **ab** + **B** or via the reaction **db** + **A**. We briefly consider the pathways for **ab** + 2**B** starting from **ba-com** + **B**, and the schematic potential energy profiles are shown in Figure 7. There are a large number of molecular complexes resulting from direct interactions between **ba-com** and **B** in all possible orientations. We selected 10 low-energy complexes within ∼10 kcal/mol which act as preassociation structures for H_2 release, including the complex **comB1-s3** discussed above. They basically involve the bridged B−H−B bonds between B of free **B** with H's belonging to both BH_3 moieties of **ba-com**. The shape and selected geometrical parameters of these complexes are summarized in Figure S3 of the Supporting Information. Table S3 of the Supporting Information lists the relative energies of the stationary points considered for this system at three levels of theory.

The complexes can be classified on the basis of the attachment position of the free boranes, their orientation, and their relative energy. The most important factor is the attachment position in such a way that both complexes **comB1** and **comB2** can be distinguished from each other. **B1** denotes an attachment of the B atom of free **B** to the BH bonds surrounding the terminal B1 atom of **ba-com**, and **B2** denotes an attachment to the central B2 atom. The letters **s** and **o** indicate the orientation of **B** in the resulting complex; **s** corresponds to the disposition of both terminal BH_3 and NH_3 groups at the *same side* (cis configuration) with respect to the central B1−B2 groups, **o** corresponds to a disposition at the *opposite side* (trans configuration), and the numbers 1, 2, 3 refer to the relative energy ordering.

The class of complexes **comB1-s** is formed by attachment of B (in free **B**) to H atoms on the same side as NH_3. This class includes four complexes, **comB1-s1**, **comB1-s2**, **comB1-s3**, and **comB1-s4**, calculated from 8.2 to 9.2 kcal/mol above the reference point **db** + **ab**. As expected, the difference in their energies is small corresponding to small variations in the position of the added **B** moiety. This is illustrated by a difference of 45−70° in the BBNB dihedral angles between **comB1-s1** (31.5°), **comB1-s2** (−13.5°), **comB1-s3** (32.6°), and **comB1-s4** (−37.7°). The variations of H-bridged bond distances and angles in these complexes are small, with a maximal change of 0.007 Å in bond distances and 1.1° in bond angles. With respect to **ba-com** + **B**, **comB1-s1** is the most stable complex. The four complexes **comB1-o*n***, n = 1, 2, 3, and 4, having a trans configuration, are consistently less stable, with energies ranging from 13.4 to 14.9 kcal/mol above the reference. This result points out the substantial stabilizing interactions between the terminal H(BH_3) and H(NH_3) atoms in the cis complexes **comB1-s**.

The second class of complexes is characterized by the H-bridged bond between B(**B**) with H(B2). Only two complexes **comB2-s** and **comB2-o** were located, 10.9 and 11.2 kcal/mol above the reference state, but 8.6 and 8.3 kcal/mol below **ba-com** + **B**, respectively. Formation of two opposite B−H−B bridged bonds makes the molecular system more symmetric. Despite the fact that some BH/HN interactions are present in **com-B2**, they are ∼2 kcal/mol higher in energy than **com-B1**.

Figure 7 shows that there is a spectrum of prereaction complexes formed from the interaction of **ba-com** with **B** with a range of complexation energies from ∼5 to ∼11 kcal/mol. Their interconversion is likely to be a facile process resulting from rotation of **B** around **ba-com** in such a way that each moiety can undergo H_2 release through the lowest-lying TS. From these complexes, we located a number of TSs for H_2 release. Their shape, main geometrical parameters, and the relative energies are shown in Figure S4 of the Supporting Information.

Different TSs denoted as **tslew** and **tsBN** have been located connecting to the class of complexes **com-B1**. Each complex is connected with one of these TSs. As above, a **tslew** characterizes a TS in which both the H(B) and H(N) atoms of the original BH_3NH_3 component contribute to the departing H_2. In such a TS, the remaining component BH_2HBH_3 plays the role of a classical Lewis acid, and the interaction takes place via bridged B−H−B bonds. Again, a TS **tsBN** has the same feature as **tsba-BN** discussed above, but in this case either one or two BH_3 group(s) can actively take part in the H_2 formation by giving and receiving H atoms.

The TSs derived from **com-B1-s1** are **comB1-s1-tslew1** and **comB1-s1-tslew2** and have the same framework for H_2 release but differ from each other only by the position of the B1−B group. Their relative energy positions are high. These pathways are much less favored than many of those discussed above. **comB1-s1-tsBN1** is characterized by an eight-member cyclic B−H−B−H−B−H−H−N structure with participation of a BH_2HBH_3 group in the H-transfer. Thus, one H is donated from B while another H is transferred to B1. In contrast, **comB1-s1-tsBN2** contains only a six-member ring as in **tsba-BN**. The second BH_3 molecule interacts from outside and does not take part in the H_2 generation. Both TSs connect to the same products BH_2NH_2 + H_2 + B_2H_6 with much lower relative energies than the energies of the two TSs labeled **tslew**. Similar features can be found for the TSs connecting the complexes **comB1-s2**, **comB1-s3**, **comB1-s4**, **comB1-o1**, **comB1-o2**, **comB1-o3**, and **comB1-o4**. In most cases, the **tslew**'s are in the range of 58−61 kcal/mol, whereas the **tsBN**s are about 32−40 kcal/mol above the reactant reference **db** + **ab** (Figure 7).

A **tslew** and a **tsBN** have been found for each of the **s** or **o** conformers of the **comB2** complexes. In both **comB2-s-tslew** and **comB2-o-tslew**, the H_2 departs from the central BH_3NH_3 moiety, from which two BH_3 molecules interact with two remaining BH bonds. The relative energies for **tslew**'s derived from **comB2** are slightly higher than those connecting **comB1**.

With reference to the separated **ab** + 2**B** system (36.5 kcal/mol above the reference point **db** + **ab**) the TSs **tslew** are ∼21−22 kcal/mol higher in energy. These values can be compared with the energy barrier for H_2 loss of 36.8 kcal/mol in the monomer **ab**[19] or that of 26.8 kcal/mol in **ab** + **B** via **tsba-lewBB** (Figure 3). The second borane molecule induces a small additional effect in this type of TS, in comparison to the effect produced by the first borane, i.e., the beneficial interaction with the **ab** monomer is mostly contributed by the first borane.

comB2-s-tsBN and **comB2-o-tsBN** also belong to the TS class **tsBN**, but their main characteristic is that, besides having a six-member cycle as in **tsba-BN**, the second borane is attached to the BH_3 of BH_3NH_3 in such a way that the B2−B group now has two bridge B−H−B bonds. Due to this extra diborane-type stabilization, these TSs become much lower in energy, 27−28 kcal/mol relative to **db** + **ab**, 16−17 kcal/mol above

the complex **comB2**, and only 7−8 kcal/mol above the point **ba-com** + **B**. The TSs are actually 9−10 kcal/mol *below* the reactant asymptote with two separated borane molecules **ab** + 2**B**. The TSs of the **comB1-s-tsBN** family are also found to be located at ∼1−3 kcal/mol *below* the separated asymptote **ab** + 2**B**.

As discussed above, complex **comB1-s3** is also the intermediate connecting **dbab-c1** with the products $B_2H_6 + BH_2NH_2 + H_2$ (Figure 6). Thus, owing to the diversity of conformations and orientations, the complexes **comB1** and **comB2** are a point of convergence of three different entrance channels on the PES before the supersystem undergoes H_2 elimination.

tsba-BN is 23.9 kcal/mol above **ba-com** (Figure 3), and **comB2-s-tsBN** is 16.1 kcal/mol above **comB2-s** so that the interaction of the second borane leads to a reduction of 7.8 kcal/mol on the barrier height. The participation of a second borane molecule reduces the energy barrier for H_2 release from ammonia borane by more than that if just one borane is present. Taken together, the calculated results shown in Figure 7 suggest that the starting **ab** + 2**B** system can lead to spontaneous H_2 release via the TSs **comB2-tsBN** and **comB1-tsBN**.

The product $B_2H_5NH_2BH_3 + H_2$ formed from TS **comB2-s-tsBN** and its different conformers is calculated to be ∼9−10 kcal/mol above the reactants **db** + **ab** and has nearly the same energy content as the complexes **comB2** (Figure 7). The product $B_2H_5NH_2BH_3$ is an isomer of ammonia triborane ($B_3H_7NH_3$) and is 15.6 kcal/mol above the most stable form of $B_3H_7NH_3$.[20] The addition of H_2 to $B_2H_5NH_2BH_3$ is characterized by an energy barrier of 17.1 kcal/mol through TS **comB2-s-tsBN**.

Concluding Remarks

Electronic structure calculations at the CCSD(T)/aug-cc-pVTZ level have been used to study the PESs related to hydrogen release in the reactions of diborane with ammonia ($B_2H_6 + NH_3$) and ammonia borane ($B_2H_6 + BH_3NH_3$). Starting from $B_2H_6 + NH_3$, the initial steps lead to a stable $H_3BHBH_2NH_3$ adduct **ba-com**, which is also formed from condensation of ammonia borane with borane ($BH_3NH_3 + BH_3$). From this common intermediate, six TSs for H_2 loss have been located with energy barriers ranging from 18 to 93 kcal/mol relative to the reactants. The lowest-lying TS **tsba-BN** is characterized as a six-member cycle in which BH_3 exerts a bifunctional catalytic effect favoring the H_2 generation within a B−H−H−N framework. In the processes starting from $B_2H_6 + BH_3NH_3$, the diborane molecule induces a slight reduction in the energy barrier. An effective catalytic effect takes place through a comparable six-member cyclic TS with B−H−H−N transfer. The corresponding TS is ∼36 kcal/mol above the separated reactants. The behavior of two separated borane molecules is more complex involving multiple preassociation complexes and TSs. Some of the pathways are beneficial with a substantial decrease of barrier heights. Different channels from either diborane or borane appear to converge to complexes comprised of the adduct **ba-com** interacting with borane at different positions and orientations. The complexation energies range from 5 to 11 kcal/mol. Classical Lewis-type interactions of boranes with the TS of the monomer BH_3NH_3 are not important. Participation of both borane molecules in a six-member cyclic TS reduces the energy barrier to 8 kcal/mol (relative to **ba-com** + **B**), which is more efficient than interaction of borane with the BH_3 of ammonia borane in **tsba-BN** leading to a diborane type of bonding. The corresponding energy barrier is now ∼8 kcal/mol relative to the same asymptote **ba-com** + **B**. These TSs are from 1 to 9 kcal/mol *below* the separated reactant $BH_3NH_3 + 2BH_3$ (**ab** + 2**B**) asymptote, suggesting that, under thermal conditions, if ammonia borane interacts with two free borane molecules spontaneous H_2 release could occur. The present results confirm the efficient action of both borane and diborane molecules as bifunctional catalysts for H_2 release. H_2 regeneration of the $B_2H_5NH_2BH_3$ product is possible due to the near thermoneutrality of the $B_2H_6 + BH_3NH_3$ reaction and an energy barrier for H_2 addition of ∼17 kcal/mol.

Acknowledgment. Funding was provided in part by the Department of Energy, Office of Energy Efficiency and Renewable Energy under the Hydrogen Storage Grand Challenge, Solicitation No. DE-PS36-03GO93013. This work was done as part of the Chemical Hydrogen Storage Center. D.A.D. is indebted to the Robert Ramsay Endowment of the University of Alabama. V.S.N. thanks the Belgian Technical Cooperation Agency (BTC) for a doctoral scholarship. M.T.N. is indebted to the FWO-Vlaanderen for supporting his sabbatical leave at the University of Alabama.

Supporting Information Available: Tables of total energies and zero-point energies of equilibrium structures, transition states, and products, and imaginary frequencies of the transition structures, for the pathways of H_2 release from $B_2H_6 + NH_3$ (**db** + **A**), $B_2H_6 + BH_3NH_3$ (**db** + **ab**), and $BH_3NH_3 + 2BH_3$ (**ab** + 2**B**) and geometries of the structures of the stationary points optimized at the MP2/aug-cc-pVTZ level in Cartesian coordinates (Å); relative energies in kcal/mol of the stationary points for the H_2 release from $B_2H_6 + NH_3$ (**db** + **A**) and from $B_2H_6 + BH_3NH_3$ (**db** + **ab**) for Figures 3, 6, and 7 at the MP2/aVDZ, CCSD(T)/aVDZ, and CCSD(T)/aVTZ levels of calculation; figures of the energy profiles reported by McKee calculated at the MP4/6-31+G(2d,p)//MP2(6-31G(d) + ZPE level; the six-member cyclic TS optimized by Sakai at the MP2/6-31G(d,p) level; selected MP2/aVTZ geometrical parameters of different complexes **comB1-s1**, **comB1-s2**, **comB1-s3**, **comB1-s4**, **comB1-o1**, **comB1-o2**, **comB1-o3**, **comB1-o4**, **comB2-s**, and **comB2-o**; and selected MP2/aVTZ geometrical parameters of transition state structures for H_2 elimination from different complexes **comB1-s*n*** and **comB1-o*n*** ($n = 1-4$) and **comB2-s**, **comB2-o**. This material is available free of charge via the Internet at http://pubs.acs.org.

References and Notes

(1) Stock, A. *Hydrides of Boron and Silicon*; Cornell University Press: Ithaca, NY, 1933; pp 51−59.
(2) Lipscomb, W. N. *Boron Hydrides*; W. A. Benjamin Inc.: New York, 1963.
(3) Stock, A.; Kuss, E. *Chem. Ber.* **1923**, *56B*, 789.
(4) Stock, A.; Pohland, E. *Chem. Ber.* **1926**, *59B*, 2215.
(5) Stock, A.; Wierl, R. *Z. Anorg. Allg. Chem.* **1931**, *203*, 228.
(6) Schlesinger, H. I.; Burg, A. B. *J. Am. Chem. Soc.* **1936**, *58*, 409.
(7) Wiberg, E. *Z. Anorg. Allg. Chem.* **1926**, *173*, 210.
(8) (a) Schlesinger, H. I.; Burg, A. B. *J. Am. Chem. Soc.* **1938**, *60*, 290. (b) Schlesinger, H. I.; Ritter, D. M.; Burg, A. B. *J. Am. Chem. Soc.* **1938**, *60*, 1296.
(9) Schlesinger, H. I.; Ritter, D. M.; Burg, A. B. *J. Am. Chem. Soc.* **1938**, *60*, 2297.
(10) (a) Adams, A. C.; Capio, C. C. *J. Electrochem. Soc.* **1980**, *127*, 339. (b) Dworschak, W.; Jung, K.; Erhardt, H. *Thin Solid Films* **1995**, *254*, 65. (c) Andujar, J. L.; Bertran, E.; Polo, M. C. *J. Vac. Sci. Technol., A* **1998**, *16*, 578.
(11) (a) Gómez-Aleixandre, C.; Díaz, D.; Orgaz, F.; Albella, J. M. *J. Phys. Chem.* **1993**, *97*, 11043. (b) Gómez-Aleixandre, C.; Essafti, A.; Fernandez, M.; Fierro, J. L. G.; Albella, J. M. *J. Phys. Chem.* **1996**, *100*, 2148.
(12) Franz, D.; Hollenstein, M.; Hollenstein, Ch. *Thin Solid Films* **2000**, *379*, 37.

(13) (a) Sugie, M.; Takeo, H.; Matsumura, C. *Chem. Phys. Lett.* **1979**, *64*, 573. (b) Sugie, M.; Takeo, H.; Matsumura, C. *J. Mol. Spectrosc.* **1987**, *123*, 286.

(14) Carpenter, J. D.; Ault, B. S. *J. Phys. Chem.* **1991**, *95*, 3502.

(15) McKee, M. L. *J. Phys. Chem.* **1992**, *96*, 5380.

(16) Feller, D.; Dixon, D. A.; Peterson, K. A. *J. Phys. Chem. A* **1998**, *102*, 7053.

(17) Sakai, S. *Chem. Phys. Lett.* **1994**, *217*, 288.

(18) Sakai, S. *J. Phys. Chem.* **1995**, *99*, 9080.

(19) Nguyen, M. T.; Nguyen, V. S.; Matus, M. H.; Gopakumar, G.; Dixon, D. A. *J. Phys. Chem. A* **2007**, *111*, 679.

(20) Nguyen, V. S.; Matus, M. H.; Nguyen, M. T.; Dixon, D. A. *J. Phys. Chem. C* **2007**, *111*, 9603.

(21) Parry, R. W.; Schultz, D. R.; Girardot, P. R. *J. Am. Chem. Soc.* **1958**, *80*, 1.

(22) Sorokin, V. P.; Vesnina, B. I.; Klimova, N. S. *Russ. J. Inorg. Chem.* **1963**, *8*, 32.

(23) (a) Geanangel, R. A.; Wendlandt, W. W. *Thermochim. Acta* **1985**, *86*, 375. (b) Sit, V.; Geanangel, R. A.; Wendlandt, W. W. *Thermochim. Acta* **1987**, *113*, 379. (c) Wang, J. S.; Geanangel, R. A. *Inorg. Chim. Acta* **1988**, *148*, 185.

(24) (a) Wolf, G.; van Miltenburg, R. A.; Wolf, U. *Thermochim. Acta* **1998**, *317*, 111. (b) Wolf, G.; Baumann, J.; Baitalow, F.; Hoffmann, F. P. *Thermochim. Acta* **2000**, *343*, 19. (c) Baitalow, F.; Baumann, J.; Wolf, G.; Jaenicke-Rlobler, K.; Leitner, G. *Thermochim. Acta* **2002**, *391*, 159.

(25) (a) Dixon, D. A.; Gutowski, M. *J. Phys. Chem. A* **2005**, *109*, 5129. (b) Grant, D. J.; Dixon, D. A. *J. Phys. Chem. A* **2005**, *109*, 10138. (c) Matus, M. H.; Anderson, K. D.; Camaioni, D. M.; Autrey, S. T.; Dixon, D. A. *J. Phys. Chem. A* **2007**, *111*, 4411. (d) Stephans, F. H.; Baker, R. T.; Matus, M. H.; Grant, D. J.; Dixon, D. A. *Angew. Chem., Int. Ed.* **2007**, *46*, 746. (e) Nguyen, M. T.; Matus, M. H.; Dixon, D. A. *Inorg. Chem.* **2007**, *46*, 7561.

(26) (a) Stephens, F. H.; Pons, V.; Baker, R. T. *Dalton Trans.* **2007**, 2613. (b) Marder, T. B. *Angew. Chem., Int. Ed.* **2007**, *46*, 8116.

(27) Keller, P. C.; Knapp, K. K.; Rund, J. V. *Inorg. Chem.* **1985**, *24*, 2382.

(28) Frisch, M. J.; Trucks, G. W.; Schlegel, H. B.; Scuseria, G. E.; Robb, M. A.; Cheeseman, J. R.; Montgomery, J. A., Jr.; Vreven, T.; Kudin, K. N.; Burant, J. C.; Millam, J. M.; Iyengar, S. S.; Tomasi, J.; Barone, V.; Mennucci, B.; Cossi, M.; Scalmani, G.; Rega, N.; Petersson, G. A.; Nakatsuji, H.; Hada, M.; Ehara, M.; Toyota, K.; Fukuda, R.; Hasegawa, J.; Ishida, M.; Nakajima, T.; Honda, Y.; Kitao, O.; Nakai, H.; Klene, M.; Li, X.; Knox, J. E.; Hratchian, H. P.; Cross, J. B.; Bakken, V.; Adamo, C.; Jaramillo, J.; Gomperts, R.; Stratmann, R. E.; Yazyev, O.; Austin, A. J.; Cammi, R.; Pomelli, C.; Ochterski, J. W.; Ayala, P. Y.; Morokuma, K.; Voth, G. A.; Salvador, P.; Dannenberg, J. J.; Zakrzewski, V. G.; Dapprich, S.; Daniels, A. D.; Strain, M. C.; Farkas, O.; Malick, D. K.; Rabuck, A. D.; Raghavachari, K.; Foresman, J. B.; Ortiz, J. V.; Cui, Q.; Baboul, A. G.; Clifford, S.; Cioslowski, J.; Stefanov, B. B.; Liu, G.; Liashenko, A.; Piskorz, P.; Komaromi, I.; Martin, R. L.; Fox, D. J.; Keith, T.; Al-Laham, M. A.; Peng, C. Y.; Nanayakkara, A.; Challacombe, M.; Gill, P. M. W.; Johnson, B.; Chen, W.; Wong, M. W.; Gonzalez, C.; Pople, J. A. *Gaussian 03*, revision C.01; Gaussian, Inc.: Wallingford, CT, 2004.

(29) *MOLPRO*, a package of ab initio programs designed by Werner, H.-J. and Knowles, P. J., version 2002.6; Amos, R. D.; Bernhardsson, A.; Berning, A.; Celani, P.; Cooper, D. L.; Deegan, M. J. O.; Dobbyn, A. J.; Eckert, F.; Hampel, C.; Hetzer, G.; Knowles, P. J.; Korona, T.; Lindh, R.; Lloyd, A. W.; McNicholas, S. J.; Manby, F. R.; Meyer, W.; Mura, M. E.; Nicklass, A.; Palmieri, P.; Pitzer, R.; Rauhut, G.; Schütz, M.; Schumann, U.; Stoll, H.; Stone, A. J.; Tarroni, R.; Thorsteinsson, T.; Werner, H.-J.

(30) Pople, J. A.; Seeger, R.; Krishnan, R. *Int. J. Quantum Chem., Quantum Chem. Symp.* **1977**, *11*, 149.

(31) (a) Dunning, T. H., Jr. *J. Chem. Phys.* **1989**, *90*, 1007. (b) Kendall, R. A.; Dunning, T. H., Jr.; Harrison, R. J. *J. Chem. Phys.* **1992**, *96*, 6796.

(32) Gonzalez, C.; Schlegel, H. B. *J. Chem. Phys.* **1989**, *90*, 2154.

(33) (a) Cizek, J. *Adv. Chem. Phys.* **1969**, *14*, 35. (b) Purvis, G. D.; Bartlett, R. J. *J. Chem. Phys.* **1982**, *76*, 1910. (c) Pople, J. A.; Head-Gordon, M.; Raghavachari, K. *J. Chem. Phys.* **1987**, *87*, 5968.

(34) Shimanouchi, T. *Tables of Molecular Vibrational Frequencies Consolidated, Volume I*; NSRDS-NBS 39; National Bureau of Standards; U.S. Government Printing Office: Washington, DC, 1972.

(35) Nguyen, V. S.; Matus, M. H.; Grant, D. J.; Nguyen, M. T.; Dixon, D. A. *J. Phys. Chem. A* **2007**, *111*, 8844.

JP804714R